Supporting Information

Design and Synthesis of Luminescence Chemosensors Based on Alkynyl Phosphine Gold(I)-Copper(I) Aggregates

Xiaoming He, Nianyong Zhu and Vivian Wing-Wah Yam*

Institute of Molecular Functional Materials[†] *and Department of Chemistry, The University of Hong Kong, Pokfulam Road, Hong Kong, P.R. China.*

*To whom correspondence should be addressed. Email: wwyam@hku.hk (V. W. W. Y.)

[†]Areas of Excellence Scheme, University Grants Committee (Hong Kong)

Tables and Figures

Table S1 Crystallographic and structural determination data for **3**·CH_3OH·$2H_2O$

Empirical formula	$C_{181}H_{146}Au_6Cu_2F_{12}N_{12}O_9P_8$
Formula weight	4417.74
Temperature	301(2) K
Wavelength	0.71073 Å
Crystal system	Triclinic
Space group	$P\bar{1}$ (No. 2)
a	17.100(2) Å
b	19.025(2) Å
c	30.128(3) Å
α	84.66(2)°
β	85.14(2)°
γ	73.71(2)°
Volume	9349.4(18) $Å^3$
Z	2
Density (calculated)	1.569 mg m^{-3}
Absorption coefficient	5.048 mm^{-1}
F(000)	4296
Crystal size	0.4 mm × 0.15 mm × 0.13 mm
Theta range for data collection	1.51 to 25.68°
Index ranges	$-20 \le h \le 20$, $-23 \le k \le 23$, $-27 \le l \le 36$
Reflections collected	55813
Independent reflections	34756 [*R*(int) = 0.0363]
Completeness to $\theta = 25.68°$	97.9 %
Absorption correction	Empirical
Refinement method	Full-matrix least-squares on F^2
Data/restraints/parameters	34756 / 0 / 1765
Goodness-of-fit on F^2	1.057
Final R indices[a] [$I>2\sigma(I)$]	$R_1 = 0.0553$, $wR_2 = 0.1476$
R indices (all data)	$R_1 = 0.0953$, $wR_2 = 0.1641$
Largest diff. peak and hole	1.706 and −1.980 e $Å^{-3}$

[a] $R_{int} = \Sigma|F_o^2 - F_o^2(\text{mean})|/\Sigma[F_o^2]$, $R_1 = \Sigma||F_o| - |F_c||/\Sigma|F_o|$ and $wR_2 = \{\Sigma[w(F_o^2 - F_c^2)^2]/\Sigma[w(F_o^2)^2]\}^{1/2}$

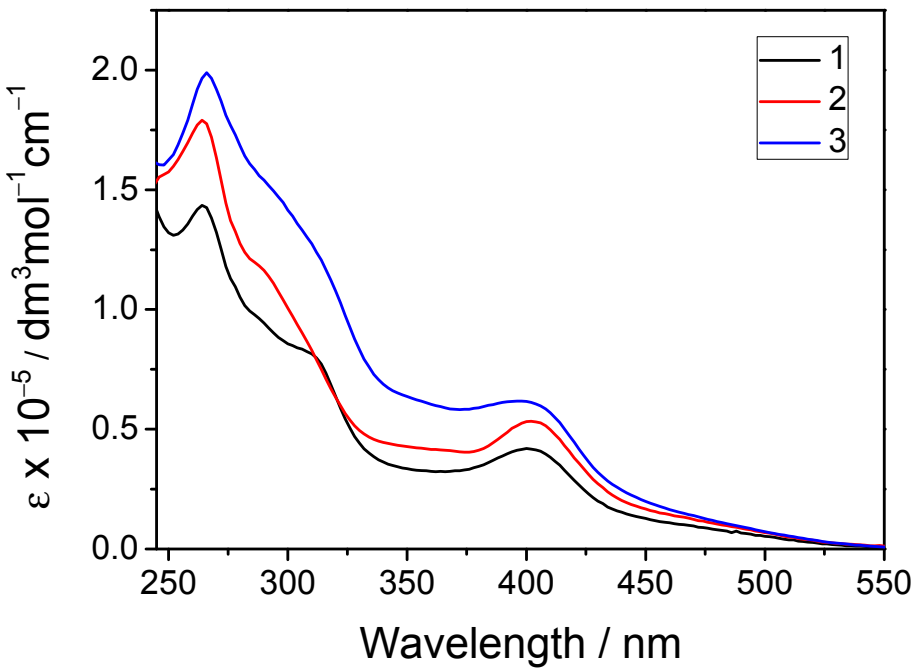

Figure S1 Electronic absorption spectra of complexes **1–3** in CH_2Cl_2 at 298 K

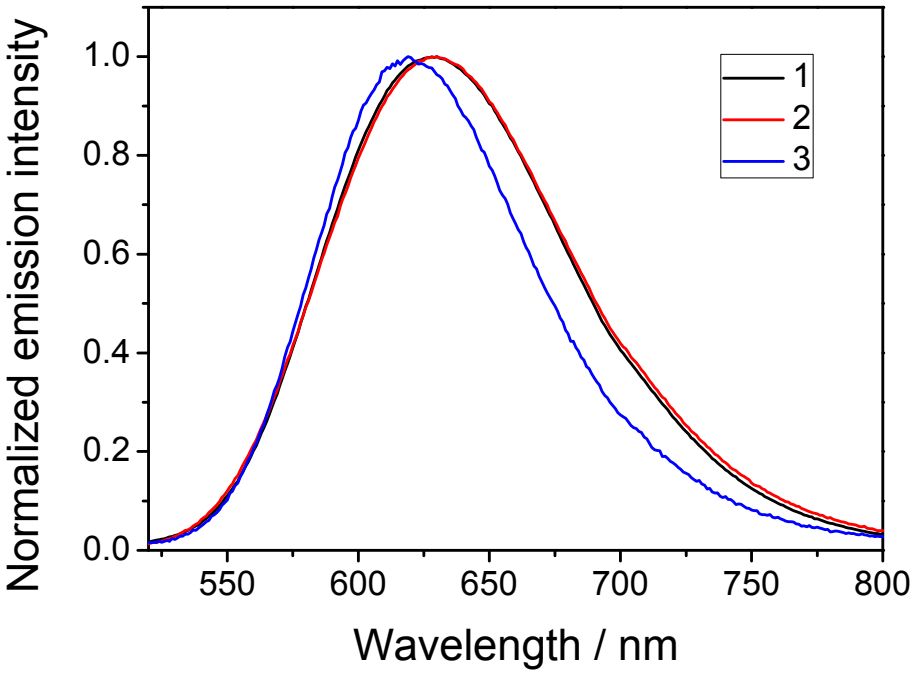

Figure S2 Electronic absorption spectra of complexes **1–3** in CH_2Cl_2 at 298 K

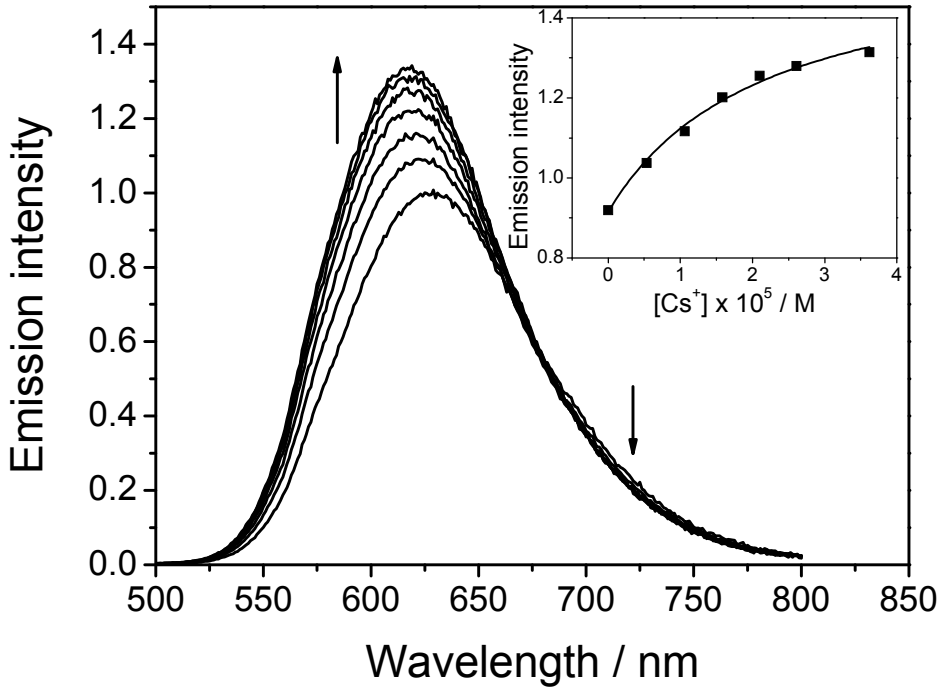

Figure S3 Emission spectral traces of **1** (2.88×10^{-7} M) in CH_2Cl_2-MeOH (1:1 v/v; 0.1 M $^nBu_4NPF_6$) upon addition of Cs^+. Excitation at 400 nm. Inset: A plot of emission intensity at 610 nm as a function of Cs^+ concentration and its theoretical fit for the 1:1 binding of complex **1** with Cs^+.

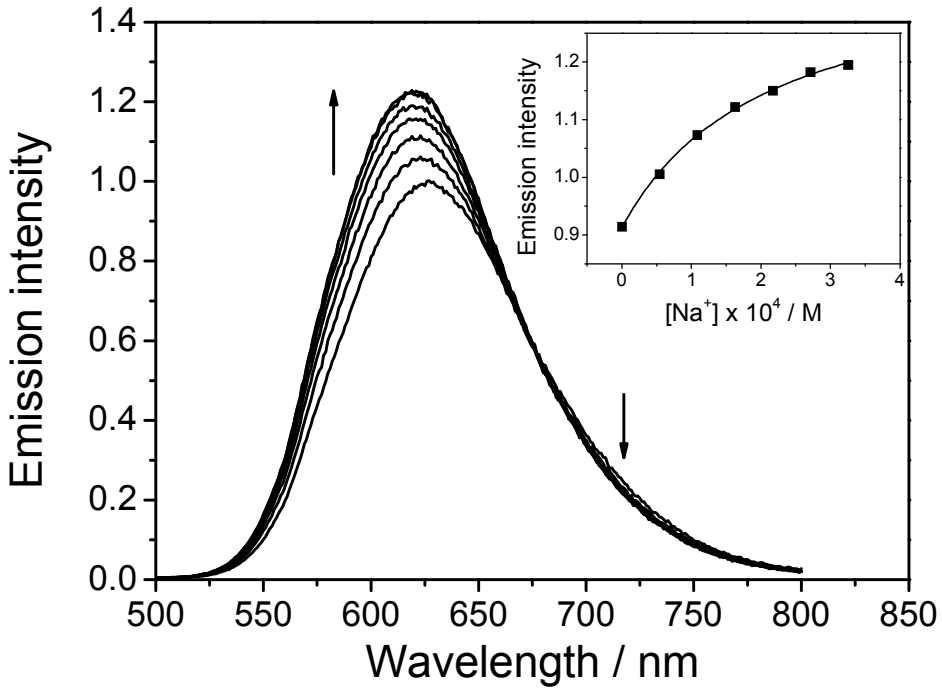

Figure S4 Emission spectral traces of **1** (2.88×10^{-7} M) in CH_2Cl_2-MeOH (1:1 v/v; 0.1 M $^{n}Bu_4NPF_6$) upon addition of Na^+. Excitation at 400 nm. Inset: A plot of emission intensity at 610 nm as a function of Na^+ concentration and its theoretical fit for the 1:1 binding of complex **1** with Na^+.

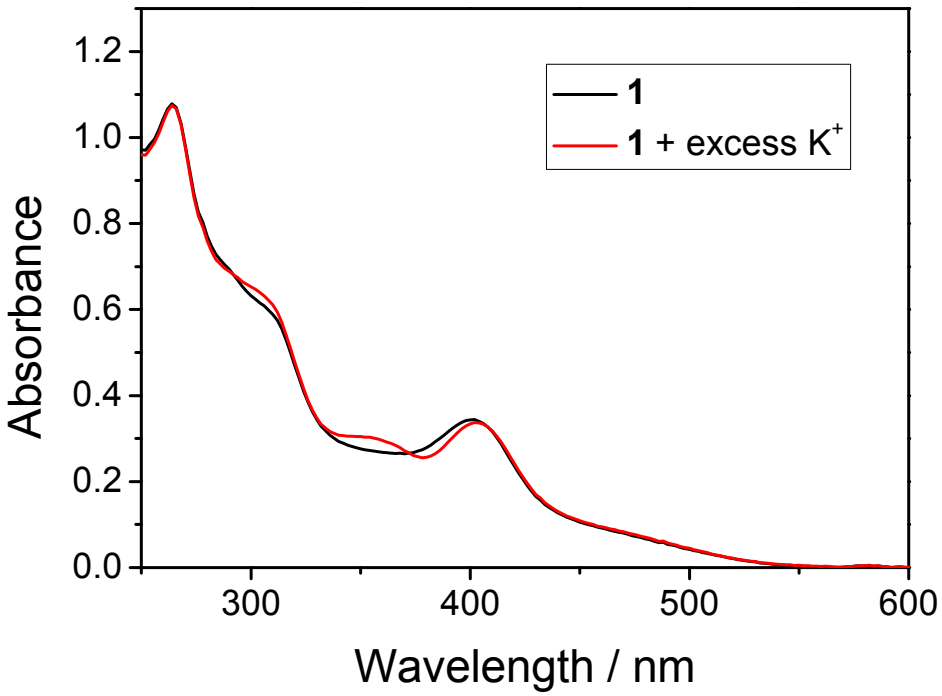

Figure S5 UV-Vis absorption spectral changes of **1** (5.76×10^{-6} M) in CH_2Cl_2-MeOH (1:1 v/v; 0.1 M $^nBu_4NPF_6$) upon addition of an excess of K^+.

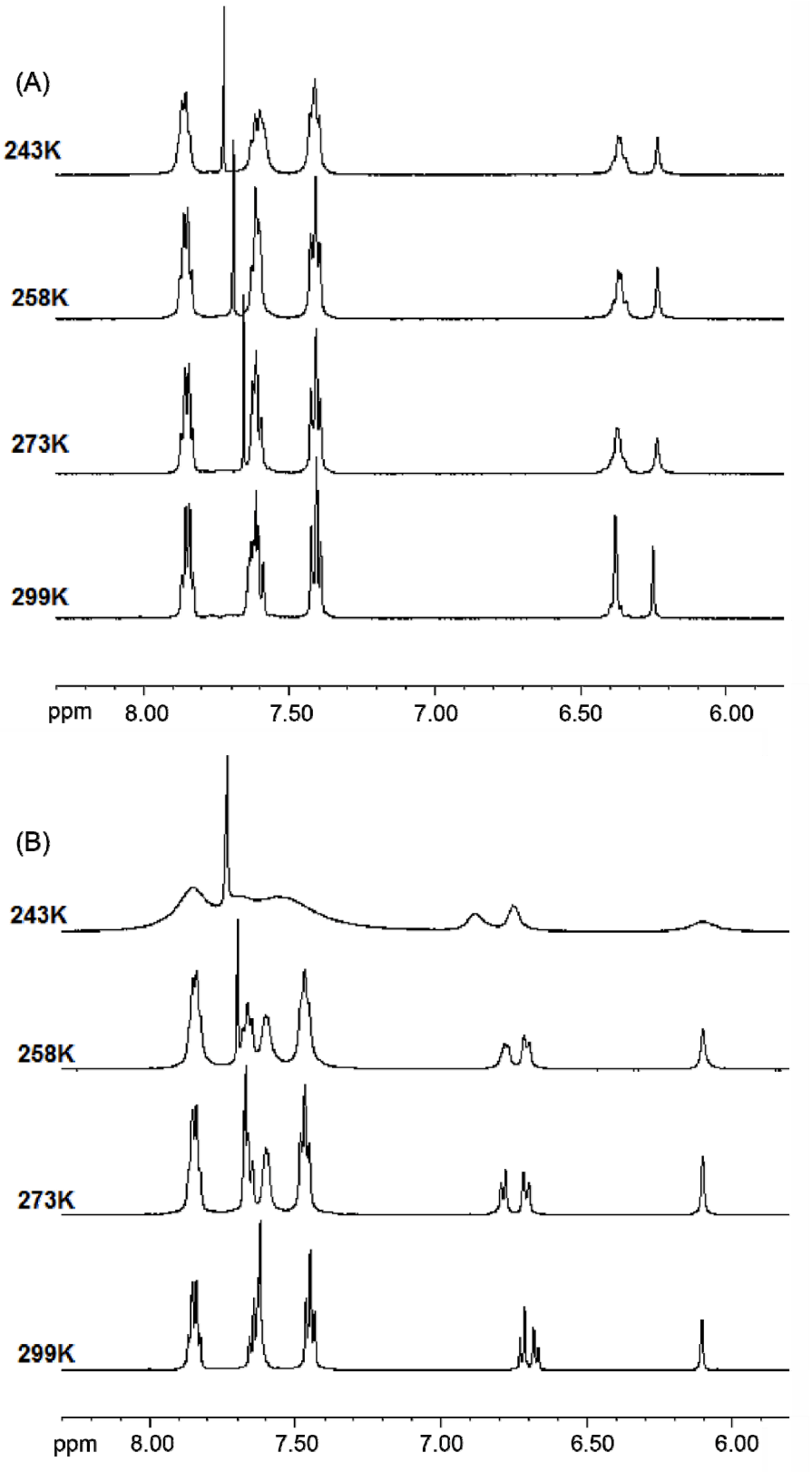

Figure S6 Variable temperature ^{1}H NMR spectra of **1** (A) in the absence and (B) in the presence of Cs^{+}.

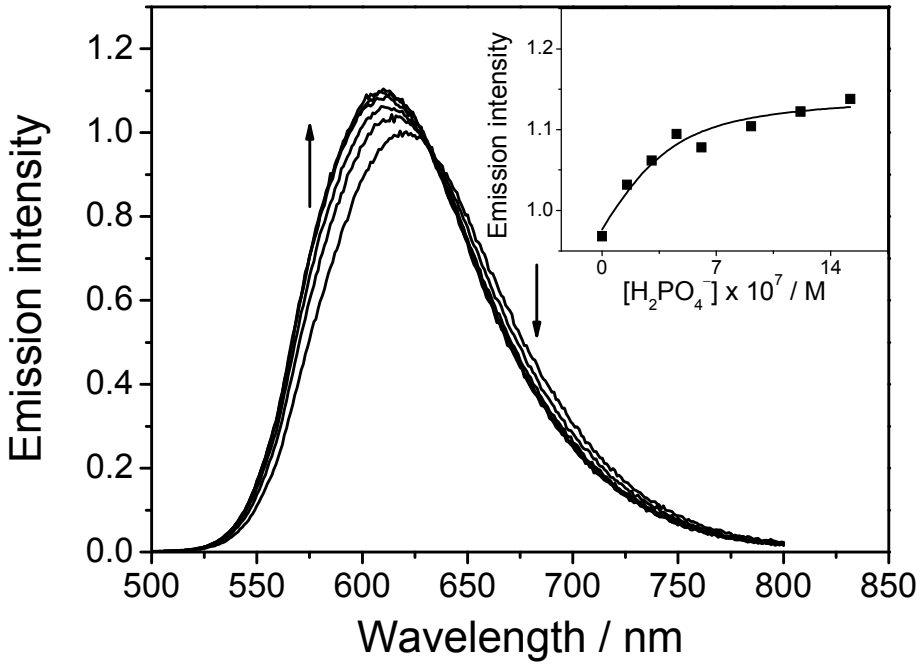

Figure S7 Emission spectral traces of **3** (3.72×10^{-7} M) in CH_2Cl_2 upon addition of $H_2PO_4^-$. Excitation at 400 nm. Inset: A plot of emission intensity at 600 nm as a function of $H_2PO_4^-$ concentration and its theoretical fit for the 1:1 binding of complex **3** with $H_2PO_4^-$.

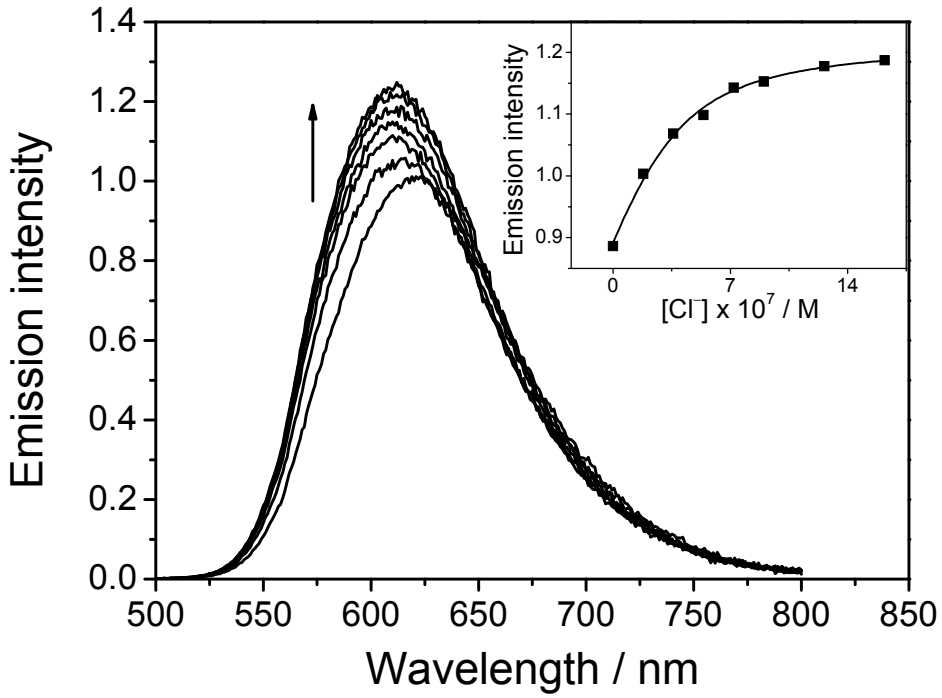

Figure S8 Emission spectral traces of **3** (3.72×10^{-7} M) in CH_2Cl_2 upon addition of Cl^-. Excitation at 400 nm. Inset: A plot of emission intensity at 600 nm as a function of Cl^- concentration and its theoretical fit for the 1:1 binding of complex **3** with Cl^-.